THE JOURNAL OF PHYSICAL CHEMISTRY A
A JOURNAL OF THE AMERICAN CHEMICAL SOCIETY

pubs.acs.org/JPCA

Article

Electronic Properties of UN and UN^- from Photoelectron Spectroscopy and Correlated Molecular Orbital Theory

Gabriel F. de Melo, Monica Vasiliu, Gaoxiang Liu, Sandra Ciborowski, Zhaoguo Zhu, Moritz Blankenhorn, Rachel Harris, Chalynette Martinez-Martinez, Maria Dipalo, Kirk A. Peterson, Kit H. Bowen,* and David A. Dixon*

Cite This: *J. Phys. Chem. A* 2022, 126, 7944−7953

Read Online

ACCESS | Metrics & More | Article Recommendations | Supporting Information

ABSTRACT: The results of calculations of the properties of the anion UN^- including electron detachment are described, which further expand our knowledge of this diatomic molecule. High-level electronic structure calculations were conducted for the UN and UN^- diatomic molecules and compared to photoelectron spectroscopy measurements. The low-lying Ω states were obtained using multireference CASPT2 including spin-orbit effects up to ~20,000 cm^{-1}. At the Feller−Peterson−Dixon (FPD) level, the adiabatic electron affinity (AEA) of UN is estimated to be 1.402 eV and the vertical detachment energy (VDE) is 1.423 eV. The assignment of the UN excited states shows good agreement with the experimental results with a VDE of 1.424 eV. An Ω = 4 ground state was obtained for UN^- which is mainly associated with the ^3H ΛS state. Thermochemical calculations estimate a bond dissociation energy (BDE) for UN^- (U^- + N) of 665.9 kJ/mol, ~15% larger than that of UN and UN^+. The NBO analysis reveals U−N triple bonds for the UN, UN^-, and UN^+ species.

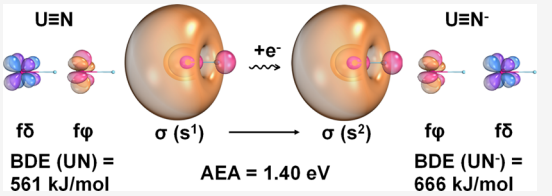

INTRODUCTION

The UN molecule has been studied by high-resolution spectroscopy,[1,2] as has UN^+. High-level electronic structure calculations of UN and UN^+ have been reported that in concert with experiments confirm that the ground state of UN is Ω = 7/2 derived mostly from a ^4H state and UN^+ is Ω = 4 derived mostly from a ^3H state. In addition, infrared matrix isolation studies of the vibrational spectrum have been reported with values of the vibrational frequency near 1000 cm^{-1}.[3,4] The bond dissociation energies (BDEs) of UN and UN^+ were predicted at the Feller−Peterson−Dixon (FPD)[5−8] composite thermochemistry level, including spin orbit corrections and high-level correlation calculations through coupled cluster CCSDTQ. The values of D_0^0 for UN and UN^+ are 134.0 and 131.5 kcal/mol, respectively. The calculated ionization energy of UN is 6.301 eV, which is in excellent agreement with the high-resolution value of 6.2987(3) eV. The SO-CASPT2/CBS calculated bond distance for UN is r_e = 1.766 Å with ω_e = 1010 cm^{-1} and for UN^+, it is r_e = 1.731 Å with ω_e = 1079 cm^{-1}. In the current work, we expand on this prior study[2] to examine the chemistry of the anion through the lens of photoelectron spectroscopy in combination with high-level electronic structure calculations building on the prior work on UN.

EXPERIMENTAL AND COMPUTATIONAL METHODS

Experimental Methods. The UN^- anions were produced and analyzed using a house-built anion photoelectron spectrometer, which has been described in detail previously.[9] The apparatus consists of an ion source, a time-of-flight mass spectrometer, a Nd: YAG photodetachment laser, and a magnetic bottle energy analyzer. The uranium nitride anions were generated in a laser vaporization ion source. A rotating, translating uranium rod was ablated using the second harmonic of a Nd: YAG laser (532 nm, 2.33 eV), while 100 PSI of N_2 gas premix (10% of N_2 in He) was expanded over the U rod. The resulting anions were then extracted with mass selection before entering the photodetachment region.

Anion photoelectron spectroscopy experiments were conducted by crossing a beam of mass-selected uranium nitride negative ions with a fixed-frequency photon beam and energy analyzing the resultant photodetached electrons. The photodetachment process is governed by the energy conservation relationship $h\upsilon$ = EBE + EKE, where $h\upsilon$ is the photon energy, EBE is the electron binding (photodetachment transition) energy, and EKE is the electron kinetic energy. The third and fourth harmonic of a Nd: YAG laser (355 nm, 3.49 eV and 266 nm, 4.66 eV) were used to photodetach electrons from the UN^- anions. The photoelectron spectra were calibrated against

Received: August 22, 2022
Revised: October 4, 2022
Published: October 21, 2022

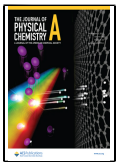

https://doi.org/10.1021/acs.jpca.2c06012
J. Phys. Chem. A 2022, 126, 7944−7953

the known transitions of Cu^-.[10] The resolution of the magnetic bottle energy analyzer is ~35 meV at 1 eV EKE.

Computational Methods. In order to interpret the photoelectron spectra of UN^-, two series of calculations were performed. First, the complete active space self-consistent field (CASSCF)[11,12] with the multireference second-order perturbation theory (CASPT2)[13,14] method was used to obtain the potential energy curves for low-lying energy Ω states. Next, the EA (electron affinity) was predicted by means of the Feller−Peterson−Dixon (FPD)[5−8] approach based on the coupled-cluster method. A detailed description of these methodologies is given in this section. These calculations were done using the MOLPRO[15,16] program package on our local UA Opteron- and Xeon-based Linux clusters.

To incorporate nondynamical correlation effects into the wavefunction, the CASSCF approach was carried out to represent each lowest-lying spin-free state, ΛS, using the aug-cc-pV*n*Z (n = D, T, Q) basis sets[17,18] for N and the cc-pV*n*Z-PP basis sets[19,20] including a 60-electron small-core pseudopotential (PP) optimized in multiconfigurational Dirac−Hartree−Fock calculations for U. These basis set combinations are denoted as a*n*-PP. The states were calculated in the highest Abelian point group available, C_{2v} for the molecules. For the molecules, the expectation values of L_z^2 were included to ensure the correct degeneracies for both components of each ΛS state. For UN, we applied the same CASSCF active space used by Heaven, Peterson, and coworkers[2] in their characterization of UN and UN^+ comprising 3 electrons in 8 orbitals (3 × a_1, 2 × b_1, 2 × b_2, 1 × a_2), which had dominant U 5f and 7s character. For UN^-, the active space of 4 electrons in the same 8 orbitals of UN resulted in a poor description of the potential energy curves; thus, the 7p orbital was also included in the active space yielding a (4/11) CASSCF (4 × a_1, 3 × b_1, 3 × b_2, 1 × a_2). For UN, 19 ΛS quartets and 20 ΛS states were calculated, while for UN^-, the ΛS manifold included 16 quintets and 13 triplets.

The relevant spin-free states that contribute to the relativistic states (Ω) were determined by considering the coupling between the lowest atomic asymptotes. In the case of UN, the coupling of U ($5f^36d^17s^2$, $^5L^o$) with N ($2s^22p^3$, $^4S^o$) yields a manifold of octets (S = 7/2) through doublets (S = 1/2). As noted by Heaven, Peterson, and coworkers,[2] octets and sextets are highly energetic and were not included in the calculation. For UN^-, the low-lying states correspond to triplets (S = 1) and quintets (S = 2) as a result of the coupling of U^- ($^6M_{13/2}$, S = 5/2) with N (S = 3/2).

Using the same active space as the preceding CASSCF, second-order perturbation theory (CASPT2)[13,14] calculations were performed to account for dynamical correlation effects. This step has multiple states calculated using a Fock operator constructed from a state-averaged density matrix, and the zeroth-order Hamiltonians for all states are constructed from the same operator. The orbitals 5s, 5p, and 5d of U and 1s of N were defined as the frozen core in the CASPT2 method, and the lowest possible IPEA[21] (Ionization Potential-Electron Affinity) shift value (0.28) was used for all states.

The spin-orbit treatment used the state interaction approach, as implemented in MOLPRO (SO-CASPT2).[22] In this method, the spin−orbit eigenstates are obtained by diagonalizing H_{el} + H_{SO} in a basis of H_{el} eigenstates. The ΛS states were state-averaged to obtain a common set of molecular orbitals. The matrix elements of H_{SO} were constructed using the spin−orbit operator from the U PP. Here, the spin−orbit matrix elements have been calculated throughout at the CASSCF level of theory using the same basis set as used for the diagonal terms, and the diagonal terms of H_{el} + H_{SO} have been replaced with CASPT2 energies. The latter energies for the two components of each molecular state with $\Lambda \neq 0$ were manually averaged when needed to ensure exact degeneracies. After diagonalization of H_{el} + H_{SO}, the values of Ω for each molecule were assigned by converting from a Cartesian eigenfunction basis to a spherical basis and then adding the projection of the spin angular momentum S on the diatomic axis, Σ, to Λ to obtain Ω.[23]

For the ground state of the diatomic, open shell calculations were performed with the R/UCCSD(T) approach where the restricted open-shell Hartree−Fock calculation is carried out followed by a relaxation of the spin constraint at the coupled cluster level.[24−27] These calculations used the third-order Douglas−Kroll−Hess Hamiltonian (DKH3)[28−30] with the aug-cc-pV*n*Z-DK basis set[18,31] for N and the cc-pwCV*n*Z-DK3 basis set for U[20]. The optimized CCSD(T) energies at n = D, T, and Q basis sets were extrapolated to the complete basis set (CBS) limit using the mixed Gaussian/exponential shown in eq 1.[32,33]

$$E_n = E_{CBS} + A \exp[-(n-1)] + B \exp[-(n-1)^2] \quad (1)$$

The potential energy curves for the diatomic were obtained at the SO-CASPT2/aQ-PP level by computing seven-single point energies distributed around the equilibrium bond length of the ground state ($r - r_e$ = −0.3, −0.2, −0.1, 0.0, +0.1, +0.3, +0.5 Bohr) optimized at the CCSD(T)/aw*n*-DK level.[34−36]

The EA of UN was obtained through additional calculations following the FPD[5−8] approach. These included contribution of the core-valence correlation (ΔE_{CV}), zero-point energies (ΔE_{ZPE}), calculated as 0.5 ω_e − 0.25 $\omega_e x_e$ with frequencies obtained from fitting the CCSD(T)/awQ-DK curve,[37] and the spin-orbit correction ΔE_{SO}, which was taken from the SO-CASPT2 calculation using the aQ-DK3[18,31] basis set, on top of the complete basis set (CBS) limit value. The Gaunt term (ΔE_{Gaunt}), which accounts for spin-other-orbit coupling, was obtained as the energy difference between Dirac−Hartree−Fock (DHF) calculations with the four-component Dirac−Coulomb (DC) and the Dirac−Coulomb−Gaunt (DCG) Hamiltonian using fully uncontracted basis sets, cc-pVDZ-DK3 on U, and aug-cc-pVDZ on N. These calculations were carried out using the DIRAC program.[38] Higher-order correlation effects were estimated using the DKH3 Hamiltonian with the MRCC[39,40] package as implemented in MOLPRO, where ΔE_T = CCSDT − CCSD(T) in aT-DK basis sets[41,42] and ΔE_Q = CCSDT(Q) − CCSDT in aD-DK basis sets.[43]

A bonding analysis of the UN and UN^- species was made through the Natural Population Analysis (NPA) results based on the Natural Bond Orbitals (NBOs)[44,45] using NBO7[46,47] with the MOLPRO program package at the aD-DK level.

RESULTS AND DISCUSSION

Photoelectron Spectrum of UN^-. Figure 1 presents the observed photoelectron spectra (PES) of the ion UN^-. Selected EBEs were assigned for four major peaks (three in the third harmonic spectrum), ranging from 1.0 to 4.0 eV, at 1.424, 2.035, 3.455, and 3.808 eV.

Electronic Structure Calculations of UN and UN^-. Low-lying electronic states of UN^- were calculated to interpret the PES spectra. The energetic order of the states and their

https://doi.org/10.1021/acs.jpca.2c06012
J. Phys. Chem. A 2022, 126, 7944−7953

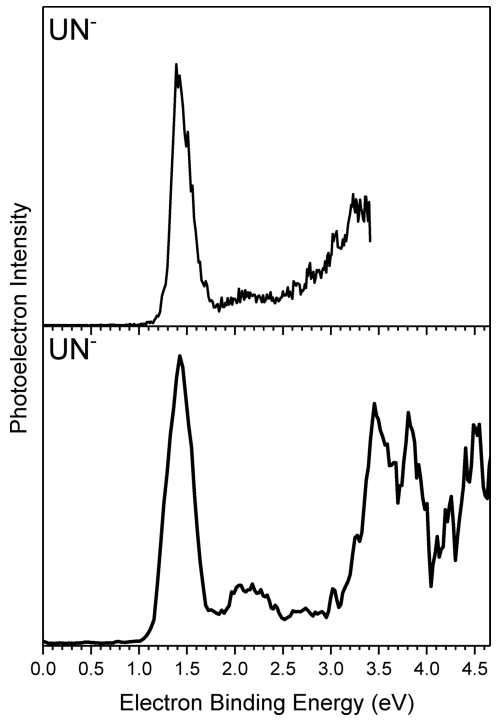

Figure 1. Photoelectron spectra of UN^- obtained using the third (355 nm) and fourth harmonic (266 nm).

interaction can help us identify possible transitions in the PES. Table 1 shows the excitation energies of the Ω states of UN^-

Table 1. Low-Lying States of UN^- at the CASPT2/aQ-PP + SO Level

state	Ω	Δ*E* (eV)	ΛS composition
$^3H_4$	4	0.000	92% ^3H + 7% $^3\Gamma$
$^3\Pi_0$	0	0.321	52% $^3\Pi$ + 48% $^3\Sigma^-$
$^3\Gamma_3$	3	0.394	77% $^3\Gamma$ + 20% $^3\Phi$
$^3\Pi_1$	1	0.419	45% $^3\Pi$ + 30% $^3\Delta$ + 25% $^3\Sigma^-$
$^3H_5$	5	0.556	92% ^3H + 8% $^3\Gamma$
$^3\Pi_2$	2	0.759	55% $^3\Pi$ + 45% $^3\Phi$
$^3\Pi_0$	0	0.812	100% $^3\Pi$
$^3\Delta_1$	1	0.860	59% $^3\Delta$ + 41% $^3\Sigma^-$
$^3\Phi_4$	4	0.867	100% $^3\Phi$
$^3\Gamma_4$	4	0.904	85% $^3\Gamma$ + 7% $^3\Phi$ + 7% ^3H
$^3H_6$	6	1.187	100% ^3H
$^3\Phi_3$	3	1.252	94% $^3\Phi$ + 5% $^3\Gamma$
$^5I_4$	4	1.254	95% ^5I + 5% ^5H
$^3\Delta_1$	1	1.314	100% $^3\Delta$
$^3\Sigma_0^-$	0	1.335	52% $^3\Sigma^-$ + 48% $^3\Pi$
$^3\Pi_1$	1	1.360	54% $^3\Pi$ + 25% $^3\Sigma^-$ + 20% $^3\Delta$
$^3\Delta_2$	2	1.368	55% $^3\Delta$ + 45% $^3\Pi$
$^3\Gamma_5$	5	1.418	92% $^3\Gamma$ + 8% ^3H
$^5\Gamma_2$	2	1.558	86% $^5\Gamma$ + 12% $^5\Phi$
$^5I_5$	5	1.576	92% ^5I + 8% ^5H
$^3\Delta_3$	3	1.602	92% $^3\Delta$ + 7% $^3\Gamma$
$^5H_3$	3	1.725	69% ^5H + 25% $^5\Gamma$ + 5% $^5\Phi$
$^5\Gamma_3$	3	1.751	56% $^5\Gamma$ + 31% ^5H + 14% $^5\Phi$
$^5\Phi_1$	1	1.790	100% $^5\Phi$
$^5I_6$	6	1.915	92% ^5I + 8% ^5H
$^5\Gamma_4$	4	1.948	76% $^5\Gamma$ + 22% $^5\Phi$

obtained at the SO-CASPT2/aQ-PP level, together with their composition based on the triplet and quintet ΛS states. To complement their characterization, Table 2 provides the

Table 2. SO-CASPT2/aQ-PP Spectroscopic Parameters for the Low-Lying Ω States of UN^-

state	T_e (cm^{-1})	r_e (Å)	ω_e (cm^{-1})	$\omega_e x_e$ (cm^{-1})	B_e (cm^{-1})
$^3H_4$	0	1.799	958.4	2.4	0.394
$^3\Pi_0$	2589	1.795	958.3	2.3	0.396
$^3\Gamma_3$	3178	1.799	950.1	2.3	0.394
$^3\Pi_1$	3379	1.796	956.4	2.3	0.395
$^3H_5$	4484	1.798	959.8	2.4	0.394
$^3\Pi_2$	6122	1.796	955.6	2.3	0.395
$^3\Pi_0$	6549	1.794	959.7	2.7	0.396
$^3\Delta_1$	6936	1.792	919.6	1.4	0.397
$^3\Phi_4$	6993	1.791	991.8	4.6	0.398
$^3\Gamma_4$	7291	1.797	951.1	0.7	0.395
$^3H_6$	9574	1.795	962.8	3.5	0.395
$^3\Phi_3$	10,098	1.788	910.4	0.1	0.399
$^5I_4$	10,114	1.791	986.4	1.1	0.398
$^3\Delta_1$	10,598	1.796	955.2	3.0	0.395
$^3\Sigma_0^-$	10,767	1.792	961.5	1.5	0.397
$^3\Pi_1$	10,969	1.792	961.0	2.5	0.397
$^3\Delta_2$	11,034	1.794	958.3	2.1	0.396
$^3\Gamma_5$	11,437	1.797	953.8	2.3	0.395
$^5\Gamma_2$	12,566	1.785	959.1	4.9	0.400
$^5I_5$	12,711	1.790	945.1	1.0	0.398
$^3\Delta_3$	12,921	1.786	960.8	2.2	0.400
$^5H_3$	13,913	1.785	951.9	2.6	0.400
$^5\Gamma_3$	14,123	1.786	957.8	3.4	0.400
$^5\Phi_1$	14,437	1.791	927.7	0.7	0.397
$^5I_6$	15,446	1.788	950.0	3.1	0.399
$^5\Gamma_4$	15,712	1.787	950.5	3.1	0.399

associated spectroscopic constants. Overall, 26 states were obtained with energy up to 2.0 eV. The ground state of UN^- is predicted to be Ω = 4 with a bond length of 1.799 Å and ω_e equal to 958.4 cm^{-1} at the SO-CASPT2 level. These results are in excellent agreement with the ones obtained at the CCSD(T)/aQ-DK level (without SO), 1.794 Å and 958.4 cm^{-1}, respectively. Based on the ΛS composition, the ground state is well described by the ^3H state. The bond lengths of the excited states deviate by only 0.014 Å from that of the ground state, yielding similar vibrational constants for all states.

Two unpaired f electrons ($f\delta$ $f\varphi$) are predicted for the electronic configuration of $^3H_4$ arising from the $5f^27s^2$ configuration of U^{2+} following an ionic model ($U^{2+}N^{3-}$). The ground state of U^{2+} has been assigned[48] as $^5I_4$ ($5f^4$). The UN^- state associated with this configuration is predicted to be 1.254 eV (10,114 cm^{-1}) higher than the ground state of UN^-. Table 1 shows that all states with energies below 1.2 eV are essentially triplet states with the quintet states having higher excitation energies. The first excited state (Ω = 0) is characterized by a strong mixing of the $^3\Pi$ and $^3\Sigma^-$ states. As the first excited state is 0.321 eV (2589 cm^{-1}) higher than the ground state, we would not expect this state to be populated and to contribute to the PES. The Ω manifold of states for UN^- is displayed in Figure 2.

Table 3 shows the low-lying Ω states of UN with their correspondent composition, and Table 4 presents their associated spectroscopic constants. Below ~20,000 cm^{-1}, we

https://doi.org/10.1021/acs.jpca.2c06012
J. Phys. Chem. A 2022, 126, 7944−7953

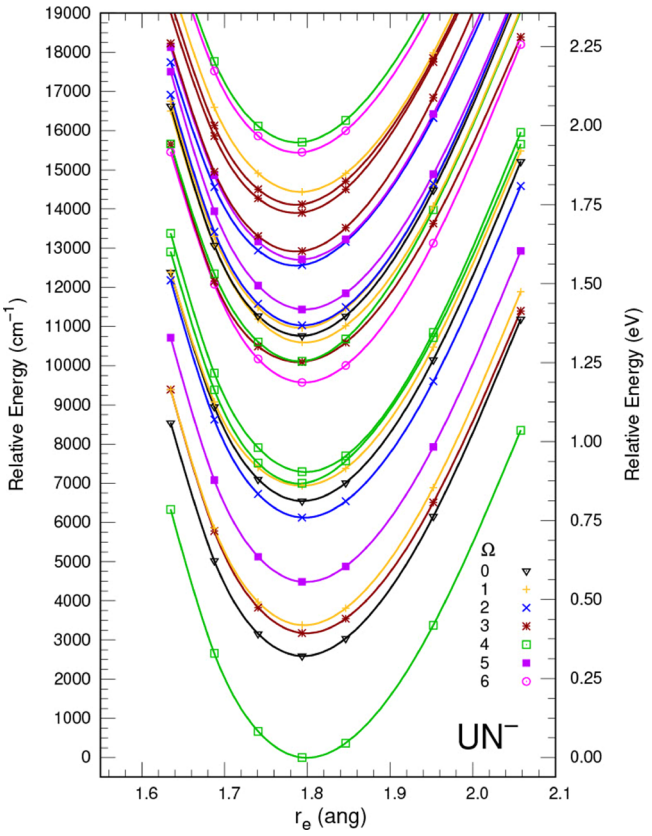

Figure 2. SO-CASPT2/aQ-PP potential energy curves for the low-lying Ω states of UN$^-$.

found 58 doublet and quartet states, all of which are derived from a $5f^27s^1$ electron configuration in contrast to the U^{3+} ($5f^3$, $^4I_{9/2}$) ground state configuration. As proposed by Matthew and Morse,[1] the $5f^27s^1$ configuration stability over the $5f^3$ configuration, as compared to the isoelectronic UO^+ ($5f^3$, $^4I_{9/2}$), might be due to the shorter internuclear distance and the greater charge of the ligand. Also, using a ligand field model, the 7s orbital results in more stability as it can be readily polarized away from N^- because of its diffuse nature. To illustrate this, Figure 3 shows the 7s (σ) and 5f orbitals ($f\delta$, $f\pi$, $f\varphi$, $f\sigma$) obtained at the the CASSCF/aD-PP level using the IboView program.[49] Thus, as shown above, the additional electron of UN$^-$ goes to the 7s orbital instead of the 5f or 6d orbitals.

The ground state of UN ($\Omega = 3.5$) is well described by the ^4H ($f\delta\ f\varphi\ \sigma$) state with minor mixtures of the $^4\Gamma$ and $^2\Gamma$ states. The calculated spectroscopic parameters show an equilibrium bond length of 1.768 Å and a vibrational frequency of 1006.0 cm^{-1}, in agreement with the calculated values by Peterson, Heaven, and coworkers[2] (1.766 Å, 1010 cm^{-1}) and the experimental r_e result of Matthew and Morse[1] (1.7650(12) Å). At the CCSD(T)/aQ-DK level, these constants are 1.762 Å and 1017.8 cm^{-1}. The first excited state, $^2H_{9/2}$ ($\sigma\ f\delta\ f\varphi$), lies only 0.056 eV (452 cm^{-1}) above the ground state and shows considerable mixing with the ^4H state. The strong mixture of ΛS states becomes more evident as we go to higher excited states. The energetic profile of the low-lying Ω states is illustrated in Figure 4. Compared to UN$^-$, appreciably more states are found in the equilibrium region, which results in a very dense manifold of states, especially above ~8000 cm^{-1}.

Electron Detachment Energies. In order to compare the calculated detachment properties with the experimental PES, additional high accuracy calculations are required. We performed calculations at the FPD level to obtain the vertical detachment energy (VDE) and the adiabatic electron affinity (AEA), as shown in Table 5. The adiabatic EA was computed as the energy difference between the ground states of UN ($^4H_{7/2}$) and UN$^-$ ($^3H_4$) and includes a small zero-point vibrational correction. For the VDE, the ground state of UN was calculated at the equilibrium bond length of UN$^-$ and the relative energy obtained without the inclusion of ΔE_{ZPE}. At the CCSD(T)/CBS level, the AEA is calculated to be 1.356 eV. Including additional corrections, the final FPD value is 1.402 eV. The computed VDE is 1.423 eV at the FPD level, only 0.021 eV greater than the AEA. Because the ΔE_{ZPE} is only 0.004 eV, at the CCSD(T)/CBS level the AEA-VDE difference is almost the same (0.025 eV). The core-valence, full triple, and full quadruple corrections to the AEA are all positive, whereas the SO correction and the QED are negative. The Gaunt correction is smaller and positive. The additional contributions to the ionization energy, IE(UN), are given in Table 5 for comparison and are, in general, of similar magnitudes, although the signs may change.

Compared to the PES, the predicted AEA and VDE are consistent with the first EBE (maxima) located at 1.424 eV. It should be noted that the first large maximum has a very broad base ranging from ~1.2 to ~1.8 eV, which could be attributed to several states. This behavior is also noted for the highest peaks of the spectrum. Thus, the assignment of the specific excited states of UN that corresponds to the observed peaks becomes difficult. We listed the calculated VDEs at the SO-CASPT2 level in Table 6 to help identify which states could account for the observed EBEs.

For the first experimental EBE at 1.424 eV, there are seven states that could be part of this peak; here, we consider a range from ~1.410 to ~1.830 eV. The second maximum, located at 2.035 eV, has a broad peak with lower intensity ranging from ~1.9 to 2.5 eV. According to our calculations, this region accommodates a total of 15 states with the $^4H_{11/2}$ state as a potential candidate for assignment. There are 20 states predicted from ~2.55 to 3.05 eV, which are consistent with the valley between the second and third EBEs. For the intense experimental peak at 3.455 eV, there are five states ($^4\Phi_{9/2}$, $^2\Sigma^+_{1/2}$, $^2\Delta_{3/2}$, $^2\Phi_{7/2}$, $^2\Delta_{5/2}$) which can account for the observed peak. In addition, eight states were obtained from ~3.1 to ~3.3 eV as part of the tail of this peak. For the next assigned experimental peak at 3.808 eV, two doublet and two quartet states are predicted to fall in this region.

Thermochemistry. The IE and BDE of UN were calculated by Heaven, Peterson, and coworkers[2] at the FPD level to be 6.292 eV (145.31 kcal/mol) and 560.5 kJ/mol, respectively. The authors also predicted $\Delta H_f^\circ{}_{0K}$ = 444.8 kJ/mol for UN. In order to obtain the BDE for UN$^-$ to the U$^-$ + N asymptote, we used the calculated EA of UN (Table 5), ΔH_f°(UN), and the experimental values for the atomic heats of formation of U$^-$ ($\Delta H_f^\circ{}_{0K}$ = 504.857 kJ/mol) and N ($\Delta H_f^\circ{}_{0K}$ = 470.579 kJ/mol) from the active thermochemical tables.[50−52] The heat of formation of U$^-$ was obtained from the experimental EA(U) of 0.309 ± 0.025 eV[9] and $\Delta H_f^\circ{}_{0K}$ of U. Using this approach, $\Delta H_f^\circ{}_{0K}$(UN$^-$) = 309.5 kJ/mol and BDE = 665.9 kJ/mol. The BDE of UN$^+$ is 550.2 kJ/mol ($\Delta H_f^\circ{}_{0K}$ = 1052.7 kJ/mol),[2] only 10 kJ/mol lower than that of the BDE(UN). Compared to UN$^-$, the bond of UN and UN$^+$ is

https://doi.org/10.1021/acs.jpca.2c06012
J. Phys. Chem. A 2022, 126, 7944−7953

Table 3. Low-Lying States of UN at the CASPT2/aQ-PP + SO Level

state	Ω	ΔE (eV)	ΛS composition
$^4H_{7/2}$	3.5	0.000	83% ^4H + 8% $^4\Gamma$ + 8% $^2\Gamma$
$^2H_{9/2}$	4.5	0.056	47% ^2H + 34% ^4H + 8% $^2\Gamma$ + 6% $^4\Gamma$
$^4\Gamma_{5/2}$	2.5	0.276	62% $^4\Gamma$ + 24% $^4\Phi$ + 6% $^2\Phi$ + 6% $^4\Delta$
$^4\Sigma^-_{1/2}$	0.5	0.283	39% $^4\Sigma^-$ + 39% $^4\Pi$ + 14% $^2\Sigma^-$ + 5% $^2\Pi$
$^2\Gamma_{7/2}$	3.5	0.352	42% $^4\Phi$ + 34% $^4\Delta$ + 11% $^4\Pi$ + 8% $^2\Delta$
$^4\Phi_{3/2}$	1.5	0.356	34% $^2\Gamma$ + 27% $^4\Gamma$ + 19% $^4\Phi$ + 8% $^2\Phi$ + 6% $^2\Phi$
$^4\Delta_{5/2}$	2.5	0.408	25% $^4\Delta$ + 22% $^2\Phi$ + 13% $^2\Delta$ + 12% $^4\Gamma$ + 10% $^4\Pi$
$^4\Sigma^-_{3/2}$	1.5	0.486	25% $^4\Sigma^-$ + 23% $^4\Pi$ + 20% $^2\Delta$ + 15% ^{2} Π + 10% $^4\Phi$
$^4\Delta_{1/2}$	0.5	0.493	40% $^4\Delta$ + 26% $^4\Pi$ + 18% $^2\Sigma^-$ + 15% $^2\Pi$
$^4H_{11/2}$	5.5	0.695	68% ^4H + 22% ^2H + 10% $^4\Gamma$
$^4H_{9/2}$	4.5	0.713	55% ^4H + 37% ^2H + 7% $^2\Gamma$
$^4\Gamma_{9/2}$	4.5	0.916	49% $^4\Gamma$ + 23% $^4\Phi$ + 14% $^2\Gamma$ + 8% ^2H + 5% ^4H
$^4\Phi_{3/2}$	1.5	0.938	78% $^4\Phi$ + 15% $^4\Delta$ + 3% $^4\Pi$
$^4\Gamma_{7/2}$	3.5	0.960	49% $^4\Gamma$ + 20% $^2\Phi$ + 14% $^2\Gamma$ + 8% ^4H
$^4\Pi_{1/2}$	0.5	0.966	44% $^4\Pi$ + 26% $^4\Delta$ + 11% $^2\Sigma^-$ + 10% $^4\Sigma^-$ + 8% $^2\Pi$
$^4\Sigma^-_{3/2}$	1.5	0.981	40% $^4\Sigma^-$ + 26% $^4\Delta$ + 14% $^4\Phi$ + 12% $^2\Delta$ + 6% $^2\Pi$
$^2\Sigma^-_{1/2}$	0.5	0.985	40% $^4\Pi$ + 36% $^4\Phi$ + 12% $^2\Delta$ + 9% $^4\Gamma$
$^4\Pi_{5/2}$	2.5	1.008	36% $^4\Delta$ + 33% $^2\Gamma$ + 30% $^4\Phi$
$^4\Delta_{7/2}$	3.5	1.020	26% $^2\Pi$ + 24% $^2\Sigma^-$ + 24% $^4\Pi$ + 13% $^4\Delta$ + 7% $^4\Sigma^-$
$^4\Pi_{1/2}$	0.5	1.034	41% $^4\Pi$ + 25% $^4\Sigma^-$ + 25% $^4\Delta$ + 4% $^4\Delta$
$^2\Pi_{3/2}$	1.5	1.043	30% $^2\Pi$ + 30% $^2\Delta$ + 19% $^4\Phi$ + 11% $^4\Pi$ + 9% $^4\Sigma$
$^2\Phi_{5/2}$	2.5	1.065	30% $^2\Phi$ + 15% $^4\Pi$ + 13% $^4\Delta$ + 13% $^2\Delta$ +10% $^4\Gamma$ + 8% $^4\Phi$
$^4\Phi_{5/2}$	2.5	1.104	62% $^4\Phi$ + 16% $^4\Delta$ + 5% $^2\Phi$ + 5% $^2\Delta$ + 4% $^2\Phi$
$^4\Pi_{3/2}$	1.5	1.141	39% $^4\Pi$ + 21% $^4\Delta$ + 16% $^4\Sigma^-$ + 12% $^4\Phi$ + 11% $^2\Delta$
$^4\Delta_{1/2}$	0.5	1.202	44% $^4\Delta$ + 39% $^4\Pi$ + 16% $^4\Sigma^-$
$^2\Gamma_{9/2}$	4.5	1.216	48% $^2\Gamma$ + 38% $^4\Phi$ + 7% $^4\Phi$ + 6% ^2H
$^4\Phi_{7/2}$	3.5	1.229	61% $^4\Phi$ + 27% $^2\Gamma$ + 6% $^4\Delta$
$^4H_{13/2}$	6.5	1.293	100% ^4H
$^2\Sigma^+_{1/2}$	0.5	1.302	26% $^2\Sigma^+$ + 23% $^4\Pi$ + 15% $^4\Pi$ + 15% $^4\Sigma^-$ + 9% $^2\Pi$ + 7% $^4\Sigma^-$
$^4\Delta_{5/2}$	2.5	1.358	44% $^4\Delta$ + 26% $^4\Pi$ + 13% $^4\Phi$ + 10% $^2\Phi$
$^2\Phi_{7/2}$	3.5	1.358	43% $^2\Phi$ + 20% $^4\Delta$ + 12% $^4\Delta$ + 7% $^2\Gamma$ + 7% $^4\Phi$ + 5% $^2\Gamma$
$^4\Pi_{5/2}$	2.5	1.362	31% $^4\Pi$ + 21% $^2\Delta$ + 13% $^2\Phi$ + 12% $^4\Pi$ + 8% $^4\Delta$ + 5% $^4\Delta$
$^4\Delta_{3/2}$	1.5	1.365	38% $^4\Delta$ + 21% $^2\Delta$ + 16% $^4\Sigma^-$ + 6% $^4\Pi$ + 5% $^4\Pi$ + 4% $^4\Phi$
$^2H_{11/2}$	5.5	1.378	62% ^2H + 31% ^4H + 7% $^4\Gamma$
$^2\Delta_{5/2}$	2.5	1.433	33% $^2\Delta$ + 31% $^2\Phi$ + 12% $^2\Delta$ + 10% $^4\Phi$ + 8% $^2\Delta$
$^4\Sigma^-_{3/2}$	1.5	1.457	37% $^4\Sigma^-$ + 29% $^2\Delta$ + 14% $^4\Pi$ + 7% $^4\Delta$ + 4% $^4\Phi$ + 3% $^2\Delta$
$^4\Pi_{1/2}$	0.5	1.487	52% $^4\Pi$ + 20% $^4\Delta$ + 14% $^4\Pi$ + 10% $^4\Sigma^-$
$^4\Gamma_{11/2}$	5.5	1.516	83% $^4\Gamma$ + 15% ^2H
$^2\Delta_{3/2}$	1.5	1.557	29% $^2\Delta$ + 25% $^4\Pi$ + 16% $^4\Sigma^-$ + 10% $^2\Pi$ + 9% $^4\Delta$ + 6% $^2\Delta$
$^4\Phi_{9/2}$	4.5	1.594	44% $^4\Phi$ + 40% $^4\Gamma$ + 12% $^2\Gamma$ + 3% ^4H
$^4\Phi_{7/2}$	3.5	1.601	25% $^4\Phi$ + 25% $^2\Gamma$ + 21% $^4\Delta$ + 11% $^4\Phi$ + 9% $^4\Delta$ + 3% $^2\Phi$
$^2\Pi_{1/2}$	0.5	1.605	25% $^2\Pi$ + 23% $^4\Pi$ + 23% $^2\Sigma^-$ + 12% $^4\Delta$ + 9% $^4\Sigma^-$ + 6% $^4\Pi$
$^4\Delta_{5/2}$	2.5	1.686	42% $^4\Delta$ + 16% $^4\Phi$ + 15% $^4\Pi$ + 9% $^4\Pi$ + 9% $^4\Sigma^-$ + 5% $^2\Delta$
$^4\Delta_{7/2}$	3.5	1.687	34% $^4\Delta$ + 23% $^4\Phi$ + 21% $^2\Gamma$ + 12% $^4\Delta$ + 6% $^4\Gamma$
$^2\Gamma_{9/2}$	4.5	1.691	63% $^2\Gamma$ + 26% $^4\Phi$ + 3% $^2\Gamma$ + 3% ^2H
$^2\Pi_{3/2}$	1.5	1.717	32% $^2\Pi$ + 23% $^2\Delta$ + 19% $^2\Delta$ + 9% $^4\Delta$ + 6% $^4\Delta$ + 5% $^2\Phi$
$^2\Sigma^+_{1/2}$	0.5	1.719	28% $^2\Sigma^+$ + 18% $^4\Pi$ + 17% $^4\Sigma^-$ + 14% $^4\Sigma^-$ + 12% $^2\Pi$ + 6% $^4\Pi$
$^4\Pi_{3/2}$	1.5	1.767	34% $^4\Pi$ + 26% $^4\Sigma^-$ + 11% $^2\Delta$ + 10% $^2\Delta$ + 9% $^4\Delta$ + 5% $^4\Pi$
$^2\Phi_{7/2}$	3.5	1.829	66% $^2\Phi$ + 10% $^2\Gamma$ + 8% $^4\Delta$ + 5% $^2\Phi$ + 5% $^4\Gamma$ + 4% $^4\Delta$
$^2\Delta_{5/2}$	2.5	1.834	49% $^2\Delta$ + 22% $^2\Phi$ + 7% $^4\Phi$ + 6% $^4\Pi$ + 5% $^2\Delta$ + 4% $^2\Delta$
$^4\Phi_{9/2}$	4.5	2.011	56% $^4\Phi$ + 42% $^2\Gamma$
$^2\Delta_{3/2}$	1.5	2.062	52% $^2\Delta$ + 16% $^4\Pi$ + 16% $^2\Gamma$ + 7% $^2\Delta$ + 3% $^4\Delta$ + 3% $^4\Sigma^-$
$^2\Sigma^+_{1/2}$	0.5	2.075	52% $^2\Sigma^+$ + 23% $^4\Sigma^-$ + 21% $^4\Pi$ + 4% $^4\Sigma^-$
$^2\Phi_{7/2}$	3.5	2.128	42% $^2\Phi$ + 26% $^4\Delta$ + 19% $^4\Phi$ + 11% $^2\Gamma$
$^2\Delta_{5/2}$	2.5	2.164	38% $^2\Delta$ + 24% $^4\Delta$ + 16% $^4\Pi$ + 13% $^2\Phi$ + 4% $^4\Phi$
$^2\Delta_{5/2}$	2.5	2.268	53% $^2\Delta$ + 27% $^2\Phi$ + 8% $^4\Pi$ + 7% $^2\Delta$
$^4\Sigma^-_{3/2}$	1.5	2.467	100% $^4\Sigma^-$

https://doi.org/10.1021/acs.jpca.2c06012
J. Phys. Chem. A 2022, 126, 7944−7953

Table 3. continued

state	Ω	ΔE (eV)	ΛS composition
$^4\Sigma^-_{1/2}$	0.5	2.469	100% $^4\Sigma^-$

Table 4. SO-CASPT2/aQ-PP Spectroscopic Parameters for the Low-Lying Ω States of UN

state	T_e (cm^{-1})	r_e (Å)	ω_e (cm^{-1})	$\omega_e x_e$ (cm^{-1})	B_e (cm^{-1})
$^4H_{7/2}$	0	1.768	1006.0	3.1	0.408
$^2H_{9/2}$	452	1.767	1005.7	3.0	0.408
$^4\Gamma_{5/2}$	2226	1.769	964.5	0.3	0.407
$^4\Sigma^-_{1/2}$	2283	1.768	1027.1	4.4	0.408
$^2\Gamma_{7/2}$	2839	1.771	971.9	0.1	0.407
$^4\Phi_{3/2}$	2871	1.769	1008.5	4.4	0.407
$^4\Delta_{5/2}$	3291	1.768	1000.1	3.5	0.408
$^4\Sigma^-_{3/2}$	3920	1.765	1002.6	3.1	0.409
$^4\Delta_{1/2}$	3976	1.765	1002.1	3.1	0.409
$^4H_{11/2}$	5606	1.766	1008.2	3.0	0.409
$^4H_{9/2}$	5751	1.766	1008.4	3.0	0.409
$^4\Gamma_{9/2}$	7388	1.768	1006.1	5.2	0.408
$^4\Phi_{3/2}$	7565	1.763	1028.9	4.7	0.410
$^4\Gamma_{7/2}$	7743	1.766	994.7	1.4	0.409
$^4\Pi_{1/2}$	7791	1.763	1008.5	3.5	0.410
$^4\Sigma^-_{3/2}$	7912	1.764	1003.7	3.1	0.410
$^2\Sigma^-_{1/2}$	7945	1.762	1005.9	2.8	0.410
$^4\Pi_{5/2}$	8130	1.765	999.2	3.7	0.409
$^4\Delta_{7/2}$	8227	1.767	1001.0	4.7	0.409
$^4\Pi_{1/2}$	8340	1.764	998.8	3.2	0.410
$^2\Pi_{3/2}$	8412	1.765	1008.0	5.4	0.409
$^2\Phi_{5/2}$	8590	1.759	1004.2	7.7	0.412
$^4\Phi_{5/2}$	8904	1.758	1051.9	7.9	0.413
$^4\Pi_{3/2}$	9203	1.763	998.8	1.3	0.410
$^4\Delta_{1/2}$	9695	1.760	1007.6	3.8	0.412
$^2\Gamma_{9/2}$	9808	1.763	1000.4	1.8	0.410
$^4\Phi_{7/2}$	9913	1.758	1013.8	3.4	0.413
$^4H_{13/2}$	10,429	1.765	1013.0	3.9	0.409
$^2\Sigma^+_{1/2}$	10,501	1.763	1004.4	2.5	0.410
$^4\Delta_{5/2}$	10,953	1.759	962.3	1.2	0.412
$^2\Phi_{7/2}$	10,953	1.762	1002.5	3.3	0.411
$^4\Pi_{5/2}$	10,985	1.764	993.8	1.0	0.410
$^4\Delta_{3/2}$	11,009	1.763	1012.4	4.6	0.410
$^2H_{11/2}$	11,114	1.764	1011.5	3.8	0.410
$^2\Delta_{5/2}$	11,558	1.758	990.3	1.2	0.412
$^4\Sigma^-_{3/2}$	11,751	1.763	998.3	3.6	0.410
$^4\Pi_{1/2}$	11,993	1.761	1004.4	3.1	0.411
$^4\Gamma_{11/2}$	12,227	1.764	1004.0	3.1	0.410
$^2\Delta_{3/2}$	12,558	1.762	1004.8	3.3	0.411
$^4\Phi_{9/2}$	12,856	1.759	972.6	2.3	0.412
$^4\Phi_{7/2}$	12,913	1.760	1036.9	7.4	0.411
$^2\Pi_{1/2}$	12,945	1.762	1036.5	4.1	0.411
$^4\Delta_{5/2}$	13,599	1.761	990.4	4.0	0.411
$^4\Delta_{7/2}$	13,607	1.764	1026.6	1.6	0.410
$^2\Gamma_{9/2}$	13,639	1.762	1012.6	3.9	0.411
$^2\Pi_{3/2}$	13,849	1.760	971.3	1.2	0.412
$^2\Sigma^+_{1/2}$	13,865	1.762	1015.4	2.3	0.411
$^4\Pi_{3/2}$	14,252	1.759	1005.8	3.3	0.412
$^2\Phi_{7/2}$	14,752	1.764	1003.2	3.5	0.410
$^2\Delta_{5/2}$	14,792	1.763	1002.0	3.1	0.410
$^4\Phi_{9/2}$	16,220	1.754	1019.8	3.0	0.414
$^2\Delta_{3/2}$	16,631	1.760	1007.5	3.1	0.412
$^2\Sigma^+_{1/2}$	16,736	1.760	1006.7	3.2	0.412
$^2\Phi_{7/2}$	17,163	1.751	1007.6	1.4	0.416
$^2\Delta_{5/2}$	17,454	1.755	992.6	2.2	0.414
$^2\Delta_{5/2}$	18,293	1.756	988.6	4.1	0.413
$^4\Sigma^-_{3/2}$	19,898	1.760	1019.4	3.2	0.412
$^4\Sigma^-_{1/2}$	19,914	1.760	1019.3	3.1	0.411

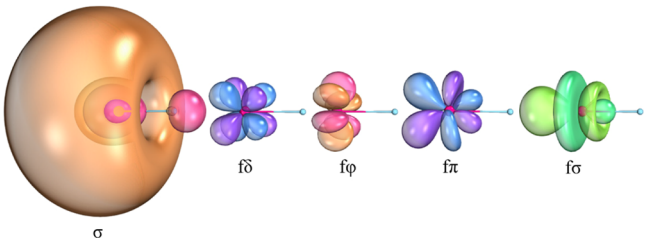

Figure 3. UN 7s (σ) and 5f (fδ, fπ, fφ, fσ) orbitals calculated at the CASSCF/aD-PP level.

~15% weaker. The heat of formation of UN^- at 298 K was calculated to be 309.2 kJ/mol using the approach described by Curtiss et al.[53] with 6.36 and 4.35 kJ/mol thermal corrections for U and N, respectively.[54] We estimate an error bar of ± 8 kJ/mol, which is mainly associated with $(\Delta H_f^\circ{}_{0K}(U))$.

Electronic Structure Analysis. The charges (q) and orbital populations from the NBO analysis are collected in Table 7 for UN, UN^-, and UN^+. The calculation for UN^+ used the optimized geometry obtained by Heaven, Peterson, and coworkers at the SO-CASPT2/CBS level.[2] Treating the UN molecule as an ionic species ($U^{3+}N^{-3}$) with a ligand field model has been shown to be a satisfactory way to predict the molecular low-lying states based on the ionic atomic states and their electronic structure. As noted above, the ground state of UN arises from the $5f^27s$ (U^{3+}) configuration. The corresponding configurations for UN^- and UN^+ are $5f^27s^2$ (U^{2+}) and $5f^2$ (U^{4+}), so all of the changes are in the 7s orbitals. UN has about +1.01 e on U and −1.01 e on N, showing ionic character, even though higher charges were not predicted. The addition of one electron decreases the U charge by ~0.8e in UN^-, whereas for UN^+, an increase in the same amount is obtained by removing one electron. There are much smaller changes for the nitrogen.

The NBO analysis provides additional insights into the nature of the UN bond. The 7s orbital populations are consistent with the configurations of UN ($7s^1$), UN^- ($7s^2$), and UN^+ ($7s^0$). Approximately 3.0 electrons were found in the 5f orbitals; there is ~1 electron in the 6d orbitals, which are different from the $5f^26d^0$ expected configuration. In all cases, there are ~2 unpaired electrons in the 5f orbitals and one paired electron in the 5f and the 6d orbitals. The paired electrons are due to backbonding from the N to the U. As a consequence, there are ~ 4.0 electrons in the N 2p orbitals. An analysis of the orbitals showed three bonding orbitals for all species with one σ and two quite polarized equivalent π bonds.

https://doi.org/10.1021/acs.jpca.2c06012
J. Phys. Chem. A 2022, 126, 7944−7953

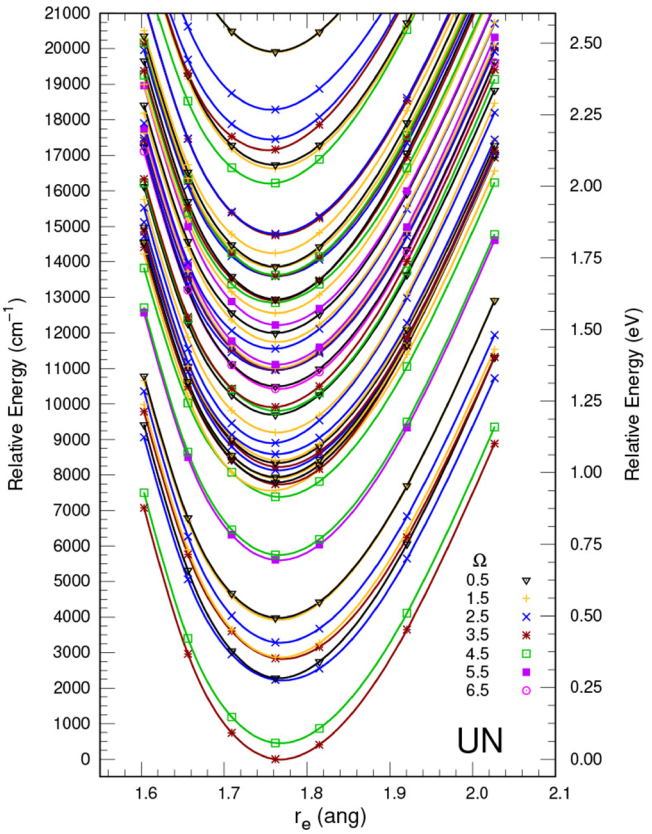

Figure 4. SO-CASPT2/aQ-PP potential energy curves for the low-lying Ω states of UN.

Table 5. FPD Components for EA(UN) (EA Defined as $-\Delta H(0\ \mathrm{K})$ for UN ($^4H_{7/2}$) + e$^-$ → UN$^-$ ($^3H_4$)) at 0 K with DK Basis Sets in eV

property	AEA	VDE[g,h]	IE[i]
awQ-DK	1.352	1.379	6.266
ΔE_{CBS}[a]	1.356	1.381	0.002
ΔE_{CV}[b]	0.021		0.023
ΔE_{ZPE}[b]	0.004		0.004
ΔE_{SO}[c]	−0.027		0.035
ΔE_{Gaunt}[d]	0.008		0.006
ΔE_{CCSDT}[e]	0.015		−0.014
ΔE_{CCSDTQ}[f]	0.032		0.009
ΔE_{QED}	−0.007		−0.019
total	1.402	1.423[h]	6.313

[a]CCSD(T) value extrapolated to the CBS limit using aw*n*-DK basis sets for *n* = D, T, Q. [b]CCSD(T)/awQ-DK. [c]SO-CASPT2 values: UN$^-$ = 0.784 eV (6321 cm^{-1}), UN = 0.811 eV (6542 cm^{-1}). [d]Fully uncontracted cc-pVDZ-DK3. [e]ΔE_T = CCSDT − CCSD(T) [f]ΔE_Q = CCSDT(Q) − CCSDT [g]UN ($^4H_{7/2}$) at UN$^-$ ($^3H_4$) geometry for each level of theory. [h]Value does not include a ZPE correction but includes the same other corrections as calculated for the AEA. [i]Ref 2.

Thus, based on the NBOs, a triple bond is expected for the UN$^{0/+/-}$ molecules built from 5f and 6d orbitals on the U and 2p orbitals on the N, respectively. Even though we can rationalize these molecules using an ionic model, contributions from covalent interactions are also relevant.

Using the values of triple bond radii of N (0.54 Å) and U (1.18 Å) by Pyykkö,[55] a bond length of 1.72 Å is predicted for the U≡N bond, which is consistent with the r_e of 1.768, 1.799, and 1.766 Å obtained for UN, UN$^-$, and UN$^+$, respectively.

Table 6. Calculated VDEs at the CASPT2/aQ-PP + SO Level (in eV)

state	VDE	state	VDE	state	VDE
$^4H_{7/2}$	1.423	$^2\Pi_{3/2}$	2.480	$^4\Phi_{9/2}$	3.031
$^2H_{9/2}$	1.482	$^2\Phi_{5/2}$	2.498	$^4\Phi_{7/2}$	3.043
$^4\Gamma_{5/2}$	1.694	$^4\Phi_{5/2}$	2.556	$^2\Pi_{1/2}$	3.049
$^4\Sigma^-_{1/2}$	1.718	$^4\Pi_{3/2}$	2.588	$^4\Delta_{5/2}$	3.119
$^2\Gamma_{7/2}$	1.772	$^4\Delta_{1/2}$	2.649	$^4\Delta_{7/2}$	3.126
$^4\Phi_{3/2}$	1.782	$^2\Gamma_{9/2}$	2.664	$^2\Gamma_{9/2}$	3.127
$^4\Delta_{5/2}$	1.834	$^4\Phi_{7/2}$	2.678	$^2\Pi_{3/2}$	3.163
$^4\Sigma^-_{3/2}$	1.921	$^4H_{13/2}$	2.719	$^2\Sigma^+_{1/2}$	3.167
$^4\Delta_{1/2}$	1.927	$^2\Sigma^+_{1/2}$	2.744	$^4\Pi_{3/2}$	3.218
$^4H_{11/2}$	2.120	$^4\Delta_{5/2}$	2.798	$^2\Phi_{7/2}$	3.261
$^4H_{9/2}$	2.140	$^2\Phi_{7/2}$	2.800	$^2\Delta_{5/2}$	3.273
$^4\Gamma_{9/2}$	2.343	$^4\Pi_{5/2}$	2.804	$^4\Phi_{9/2}$	3.467
$^4\Phi_{3/2}$	2.387	$^4\Delta_{3/2}$	2.808	$^2\Delta_{3/2}$	3.513
$^4\Gamma_{7/2}$	2.388	$^2H_{11/2}$	2.809	$^2\Sigma^+_{1/2}$	3.522
$^4\Pi_{1/2}$	2.402	$^2\Delta_{5/2}$	2.881	$^2\Phi_{7/2}$	3.584
$^4\Sigma^-_{3/2}$	2.416	$^4\Sigma^-_{3/2}$	2.903	$^2\Delta_{5/2}$	3.616
$^2\Sigma^-_{1/2}$	2.424	$^4\Pi_{1/2}$	2.936	$^2\Delta_{5/2}$	3.721
$^4\Pi_{5/2}$	2.439	$^4\Gamma_{11/2}$	2.944	$^4\Sigma^-_{3/2}$	3.950
$^4\Delta_{7/2}$	2.449	$^2\Delta_{3/2}$	3.000	$^4\Sigma^-_{1/2}$	3.952
$^4\Pi_{1/2}$	2.480				

For UN, the σ bond has mostly 5f character and the U−N π bonds have in average 47% 5f character and 53% of 6d character. With small modifications on the percentages, the bonding characters of UN are also present in UN$^-$ and UN$^+$. The bond distances are consistent with the NBO analysis and the predictions of the ground states, in that the electron changes for UN$^+$ and UN$^-$ are changes in the 7s orbital populations so that the nature of the N ligand is not substantially affected. This arises because the UN σ and π bonds have very little 7s character so that the 7s is a spectator-like orbital. This is quite different from the transition metals where the valence s orbital is often involved in the chemical bonds.

CONCLUSIONS

The combination of high-level electronic structure calculations with the PES experiments provides further insights into the U-nitrogen ligand interaction. In this work, we extend the prior study[2] of UN and UN$^+$ to obtain the electron detachment properties of UN$^-$. Potential energy curves were calculated for the excited electronic states of UN and UN$^-$ up to ∼20,000 cm^{-1} using the SO-CASPT2 method. For UN, 58 doublet and quartet states were predicted within ∼2.5 eV with a $^4H_{7/2}$ ground state and a first excited state ($^2H_{9/2}$) only 452 cm^{-1} higher in energy. In this case, a high density of states is predicted above ∼8000 cm^{-1}. Good agreement was obtained with the spectroscopic constants of the previous combined experiment/computational study.[2] UN$^-$ has a $^3H_4$ ground state, similar to that of UN$^+$, with a total of 26 states triplet and quintet states below ∼2.0 eV.

The detachment properties of UN$^-$ were studied using the FPD approach and comparison with the experimental PES showed very good agreement. The adiabatic EA(UN) is calculated to be 1.402 eV consistent with the experimental value for the first maxima of 1.424 eV. The VDE is only 0.025 eV higher than the AEA. The theoretical values include a spin-orbit correction of −0.027 eV. The PES spectrum shows four

https://doi.org/10.1021/acs.jpca.2c06012
J. Phys. Chem. A 2022, 126, 7944−7953

Table 7. NBO/HF Charges (q) and Population for $UN^{0/-/+}$ at the aD-DK Level from Molpro

property	$UN(^4H_{7/2})$	$UN^-(^3H_4)$	$UN^+(^3H_4)$
q(U)	1.009	0.205	1.852
q(N)	−1.009	−1.205	−0.852
5f (5fα/5fβ)	2.95 (2.40/0.55)	2.87 (2.38/0.49)	3.11 (2.49/0.62)
6d (6dα/6dβ)	1.20 (0.70/0.50)	1.13 (0.62/0.62)	1.15 (0.64/0.51)
7s (7sα/7sβ)	0.94 (0.91/0.03)	1.85 (0.93/0.92)	0.02 (0.01/0.01)
N 2s (2sα/2sβ)	1.85 (0.93/0.92)	1.87 (0.93/0.93)	1.88 (0.94/0.94)
N 2p (2pα/2pβ)	4.08 (2.04/2.03)	4.21 (2.10/2.10)	3.93 (1.97/1.96)

broad peaks at 1.424, 2.035, 3.455, and 3.808 eV and the assignments of the UN excited states are consistent with the experimental findings. Using the electron affinity of UN, the $\Delta H_{f\,0K}^{\circ}$ of UN^- was predicted to be 309.5 kJ/mol with a BDE(UN^-) of 665.9 kJ/mol for the $UN^- \rightarrow U^- + N$ process. The BDE(UN^-) is ∼15% higher than that of UN and UN^+.

The ground state electronic configurations of UN, UN^-, and UN^+ differ in the 7s orbital occupation. UN has a $5f^27s$ configuration on U and those for UN^- and UN^+ correspond to the $5f^27s^2$ and $5f^2$ configurations, respectively. The NBO analysis shows that the U 5f orbital population includes three electrons and the U 6d orbitals have one electron. Three U−N bonding orbitals were found, suggesting a triple U≡N bond for all three species. The increased spin-paired population in the 5f and 6d orbitals can be explained by backbonding to these orbitals from the N. Although the electronic structure and the low-lying states of $UN^{0/-/+}$ species can be rationalized by means of an ionic model, covalent interactions clearly make contributions to the bond of these systems.

■ ASSOCIATED CONTENT

Supporting Information

The Supporting Information is available free of charge at https://pubs.acs.org/doi/10.1021/acs.jpca.2c06012.

Total energies at the CCSD(T) level; complete citations for references 15, 16, 37, 39. EA; and VDE energies at awD-DK and awT-DK basis sets (PDF)

■ AUTHOR INFORMATION

Corresponding Authors

Kit H. Bowen − *Department of Chemistry, Johns Hopkins University, Baltimore, Maryland 21218, United States;* orcid.org/0000-0002-2858-6352; Email: kbowen@jhu.edu

David A. Dixon − *Department of Chemistry and Biochemistry, University of Alabama, Tuscaloosa, Alabama 35401, United States;* orcid.org/0000-0002-9492-0056; Email: dadixon@ua.edu

Authors

Gabriel F. de Melo − *Department of Chemistry and Biochemistry, University of Alabama, Tuscaloosa, Alabama 35401, United States*

Monica Vasiliu − *Department of Chemistry and Biochemistry, University of Alabama, Tuscaloosa, Alabama 35401, United States*

Gaoxiang Liu − *Department of Chemistry, Johns Hopkins University, Baltimore, Maryland 21218, United States;* orcid.org/0000-0002-1001-0064

Sandra Ciborowski − *Department of Chemistry, Johns Hopkins University, Baltimore, Maryland 21218, United States*

Zhaoguo Zhu − *Department of Chemistry, Johns Hopkins University, Baltimore, Maryland 21218, United States;* orcid.org/0000-0002-4395-9102

Moritz Blankenhorn − *Department of Chemistry, Johns Hopkins University, Baltimore, Maryland 21218, United States*

Rachel Harris − *Department of Chemistry, Johns Hopkins University, Baltimore, Maryland 21218, United States*

Chalynette Martinez-Martinez − *Department of Chemistry, Johns Hopkins University, Baltimore, Maryland 21218, United States*

Maria Dipalo − *Department of Chemistry, Johns Hopkins University, Baltimore, Maryland 21218, United States*

Kirk A. Peterson − *Department of Chemistry, Washington State University, Pullman, Washington 99164, United States;* orcid.org/0000-0003-4901-3235

Complete contact information is available at: https://pubs.acs.org/10.1021/acs.jpca.2c06012

Notes

The authors declare no competing financial interest.

■ ACKNOWLEDGMENTS

This work was supported by the U.S. Department of Energy (DOE), Office of Science, Office of Basic Energy Sciences, Heavy Element Chemistry program at Johns Hopkins University (K.H.B., experiment) through Grant Number, DE-SC0019317, at The University of Alabama (D.A.D., computational) through Grant No. DE-SC0018921, and at Washington State University (K.A.P., computational) through Grant No. DE-SC0008501. D.A.D. thanks the Robert Ramsay Fund at The University of Alabama.

■ REFERENCES

(1) Matthew, D. J.; Morse, M. D. Resonant Two-Photon Ionization Spectroscopy of Jet-Cooled UN: Determination of the Ground State. *J. Chem. Phys.* **2013**, *138*, 184303.

(2) Battey, S. R.; Bross, D. H.; Peterson, K. A.; Persinger, T. D.; Van Gundy, R. A.; Heaven, M. C. Spectroscopic and Theoretical Studies of UN and UN^+. *J. Chem. Phys.* **2020**, *152*, No. 094302.

(3) Green, D. W.; Reedy, G. T. The Identification of UN in Ar Matrices. *J. Chem. Phys.* **1976**, *65*, 2921.

(4) Hunt, R. D.; Yustein, J. T.; Andrews, L. Matrix Infrared Spectra of NUN Formed by the Insertion of Uranium Atoms into Molecular Nitrogen. *J. Chem. Phys.* **1993**, *98*, 6070.

(5) Dixon, D. A.; Feller, D.; Peterson, K. A. A Practical Guide to Reliable First Principles Computational Thermochemistry Predictions Across the Periodic Table. In *Annual Reports in Computational Chemistry*, Wheeler, R. A., Ed.; Tschumper, G. S., Section Ed.; Elsevier: Amsterdam, 2012; Vol. *8*, Ch. 1, pp. 1−28.

(6) Feller, D.; Peterson, K. A.; Dixon, D. A. Further Benchmarks of a Composite, Convergent, Statistically-Calibrated Coupled Cluster-

Based Approach for Thermochemical and Spectroscopic Studies. *Mol. Phys.* **2012**, *110*, 2381−2399.
(7) Peterson, K. A.; Feller, D.; Dixon, D. A. Chemical Accuracy in Ab Initio Thermochemistry and Spectroscopy: Current Strategies and Future Challenges. *Theor. Chem. Acc.* **2012**, *131*, 1079.
(8) Feller, D.; Peterson, K. A.; Dixon, D. A. The Impact of Larger Basis Sets and Explicitly Correlated Coupled Cluster Theory on the Feller-Peterson-Dixon Composite Method. In *Annual Reports in Computational Chemistry*, Dixon, D. A., Ed.; Elsevier: Amsterdam, 2016; Vol. *12*, pp. 47−78.
(9) Ciborowski, S. M.; Liu, G.; Blankenhorn, M.; Harris, R. M.; Marshall, M. A.; Zhu, Z.; Bowen, K. H.; Peterson, K. A. The Electron Affinity of the Uranium Atom. *J. Chem. Phys.* **2021**, *154*, 224307.
(10) Ho, J.; Ervin, K. M.; Lineberger, W. C. Photoelectron Spectroscopy of Metal Cluster Anions: Cu_n^-, Ag_n^-, and Au_n^-. *J. Chem. Phys.* **1990**, *93*, 6987−7002.
(11) Roos, B. O.; Taylor, P. R.; Siegbahn, P. E. M. A Complete Active Space SCF Method (CASSCF) Using a Density-matrix Formulated Super-CI Approach. *Chem. Phys.* **1980**, *48*, 157−173.
(12) Siegbahn, P. E. M.; Almlöf, J.; Heiberg, A.; Roos, B. O. The Complete Active Space SCF (CASSCF) Method in a Newton-Raphson Formulation with Application to the HNO Molecule. *J. Chem. Phys.* **1981**, *74*, 2384−2396.
(13) Andersson, K.; Malmqvist, P. A.; Roos, B. O.; Sadlej, A. J.; Wolinski, K. Second-Order Perturbation Theory with a CASSCF Reference Function. *J. Phys. Chem.* **1990**, *94*, 5483−5488.
(14) Andersson, K.; Malmqvist, P. A.; Roos, B. O. Second-Order Perturbation Theory with a Complete Active Space Self-Consistent Field Reference Function. *J. Chem. Phys.* **1992**, *96*, 1218−1226.
(15) Werner, H.-J.; Knowles, P. J.; Manby, F. R.; Black, J. A.; Doll, K.; Heßelmann, A.; Kats, D.; Köhn, A.; Korona, T.; Kreplin, D. A.; et al. The Molpro Quantum Chemistry Package. *J. Chem. Phys.* **2020**, *152*, 144107.
(16) Werner, H.-J.; Knowles, P. J.; Knizia, G.; Manby, F. R.; Schütz, M.; Celani, P.; Györffy, W.; Kats, D.; Korona, T.; Lindh, R.; et al. MOLPRO, version 2019.2, A Package of *Ab Initio* Programs, https://www.molpro.net (accessed January 1, 2021).
(17) Dunning, T. H., Jr. Gaussian Basis Set for Use in Correlated Molecular Calculations. I. The Atoms Boron Through Neon and Hydrogen. *J. Chem. Phys.* **1989**, *90*, 1007−1023.
(18) Kendall, R. A.; Dunning, T. H.; Harrison, R. J. Electron Affinities of the First-Row Atoms Revisited. Systematic Basis Sets and Wave Functions. *J. Chem. Phys.* **1992**, *96*, 6796−6806.
(19) Dolg, M.; Cao, X. Accurate Relativistic Small-core Pseudopotentials for Actinides. Energy Adjustment for Uranium and First Applications to Uranium Hydride. *J. Phys. Chem. A.* **2009**, *113*, 12573−12581.
(20) Peterson, K. A. Correlation Consistent Basis Sets for Actinides. I. The Th and U Atoms. *J. Chem. Phys.* **2015**, *142*, No. 074105.
(21) Ghigo, G.; Roos, B. O.; Malmqvist, P.-A. A Modified Definition of the Zeroth-Order Hamiltonian in Multiconfigurational Perturbation Theory (CASPT2). *Chem. Phys. Lett.* **2004**, *396*, 142−149.
(22) Berning, A.; Schweizer, M.; Werner, H.-J.; Knowles, P. J.; Palmieri, P. Spin-orbit Matrix Elements for Internally Contracted Multireference Configuration Interaction Wavefunctions. *Mol. Phys.* **2000**, *98*, 1823−1833.
(23) Bross, D. H. *Accurate ab initio Thermochemistry and Spectroscopy of Molecules Containing Transition Metals and Heavy Elements*, Ph.D Thesis ; Washington State University, 2015.
(24) Deegan, M. J. O.; Knowles, P. J. Perturbative Corrections to Account for Triple Excitations in Closed and Open Shell Coupled Cluster Theories. *Chem. Phys. Lett.* **1994**, *227*, 321−326.
(25) Rittby, M.; Bartlett, R. J. An Open-Shell Spin-Restricted Coupled Cluster Method: Application to Ionization Potentials in N_2. *J. Phys. Chem.* **1988**, *92*, 3033−3036.
(26) Knowles, P. J.; Hampel, C.; Werner, H.-J. Coupled Cluster Theory for High Spin, Open Shell Reference Wave Functions. *J. Chem. Phys.* **1993**, *99*, 5219−5227.
(27) Watts, J. D.; Gauss, J.; Bartlett, R. J. Coupled-Cluster Methods with Non-iterative Triple Excitations for Restricted Open-Shell Hartree-Fock and Other General Single-Determinant Reference Functions. Energies and Analytical Gradients. *J. Chem. Phys.* **1993**, *98*, 8718−8733.
(28) Douglas, M.; Kroll, N. M. Quantum Electrodynamical Corrections to the Fine Structure of Helium. *Ann. Phys.* **1974**, *82*, 89−155.
(29) Jansen, G.; Hess, B. A. Revision of the Douglas-Kroll Transformation. *Phys. Rev. A* **1989**, *39*, 6016.
(30) Wolf, A.; Reiher, M.; Hess, B. A. The Generalized Douglas-Kroll Transformation. *J. Chem. Phys.* **2002**, *117*, 9215−9226.
(31) De Jong, W. A.; Harrison, R. J.; Dixon, D. A. Parallel Douglas−Kroll Energy and Gradients in NWChem: Estimating Scalar Relativistic Effects Using Douglas−Kroll Contracted Basis Sets. *J. Chem. Phys.* **2001**, *114*, 48−53.
(32) Peterson, K. A.; Woon, D. E.; Dunning, T. H., Jr. Benchmark Calculations with Correlated Molecular Wave Functions. IV. The Classical Barrier Height of the $H+H_2 \rightarrow H_2+H$ Reaction. *J. Chem. Phys.* **1994**, *100*, 7410.
(33) Feller, D.; Peterson, K. A.; Hill, J. G. On the Effectiveness of CCSD(T) Complete Basis Set Extrapolations for Atomization Energies. *J. Chem. Phys.* **2011**, *135*, No. 044102.
(34) Purvis, G. D., III; Bartlett, R. J. A Full Coupled-Cluster Singles and Doubles Model: The Inclusion of Disconnected Triples. *J. Chem. Phys.* **1982**, *76*, 1910−1918.
(35) Raghavachari, K.; Trucks, G. W.; Pople, J. A.; Head-Gordon, M. A Fifth-order Perturbation Comparison of Electron Correlation Theories. *Chem. Phys. Lett.* **1989**, *157*, 479−483.
(36) Bartlett, R. J.; Musial, M. Coupled-Cluster Theory in Quantum Chemistry. *Rev. Mod. Phys.* **2007**, *79*, 291−352.
(37) Dunham, J. L. The Energy Levels of a Rotating Vibrator. *Phys. Rev.* **1932**, *41*, 721−731.
(38) Gomes, A. S. P.; Saue, T.; Visscher, L.; Aa Jensen, H. J.; Bast, R. DIRAC, a Relativistic Ab Initio Electronic Structure Program, Release DIRAC19, 2019, available at http://www.diracprogram.org (accessed April 25, 2022).
(39) Kállay, M.; Nagy, P. R.; Mester, D.; Gyevi-Nagy, L.; Csóka, J.; Szabó, P. B.; Rolik, Z.; Samu, G.; Csontos, J.; Hégely, B.; et al. MRCC, A Quantum Chemical Program Suite. Budapest University of Technology and Economics, Budapest. www.mrcc.hu (accessed May 1, 2022).
(40) Kállay, M.; Nagy, P. R.; Mester, D.; Rolik, Z.; Samu, G.; Csontos, J.; Csóka, J.; Szabó, P. B.; Gyevi-Nagy, L.; Hégely, B.; et al. The MRCC Program System: Accurate Quantum Chemistry from Water to Proteins. *J. Chem. Phys.* **2020**, *152*, No. 074107.
(41) Watts, J. D.; Bartlett, R. J. The Coupled-Cluster Single, Double, and Triple Excitation Model for Open-Shell Single Reference Functions. *J. Chem. Phys.* **1990**, *93*, 6104−6105.
(42) Noga, J.; Bartlett, R. J. The Full CCSDT Model for Molecular Electronic Structure. *J. Chem. Phys.* **1987**, *86*, 7041−7050.
(43) Kucharski, S. A.; Bartlett, R. J. Noniterative Energy Corrections through Fifth-Order to the Coupled Cluster Singles and Doubles Method. *J. Chem. Phys.* **1998**, *108*, 5243−5254.
(44) Reed, A. E.; Curtiss, L. A.; Weinhold, F. Intermolecular Interactions from a Natural Bond Orbital, Donor-Acceptor Viewpoint. *Chem. Rev.* **1988**, *88*, 899−926.
(45) Weinhold, F.; Landis, C. R. *Valency and Bonding: A Natural Bond Orbital Donor-Acceptor Perspective*; University Press: Cambridge, U.K., 2005.
(46) Glendening, E. D.; Landis, C. R.; Weinhold, F. NBO 7.0: New Vistas in Localized and Delocalized Chemical Bonding Theory. *J. Comput. Chem.* **2019**, *40*, 2234−2241.
(47) Glendening, E. D.; Badenhoop, J. K.; Reed, A. E.; Carpenter, J. E.; Bohmann, J. A.; Morales, C. M.; Karafiloglou, P.; Landis, C. R.; Weinhold, F. *Natural Bond Order 7.0, Theoretical Chemistry Institute*; University of Wisconsin: Madison, WI, 2018.
(48) Kramida, A.; Ralchenko, Y.; Reader, J.; NIST ASD Team. *NIST Atomic Spectra Database (ver. 5.9)*, [Online]. Available: https://

https://doi.org/10.1021/acs.jpca.2c06012
J. Phys. Chem. A 2022, 126, 7944−7953

physics.nist.gov/asd, June 15, 2022; National Institute of Standards and Technology: Gaithersburg, MD, 2021.
(49) Knizia, G. Intrinsic Atomic Orbitals: An Unbiased Bridge Between Quantum Theory and Chemical Concepts. *J. Chem. Theory Comput.* **2013**, *9*, 4834−4843.
(50) Ruscic, B.; Pinzon, R. E.; Morton, M. L.; von Laszewski, G.; Bittner, S.; Nijsure, S. G.; Amin, K. A.; Minkoff, M.; Wagner, A. F. Introduction to Active Thermochemical Tables: Several "Key" Enthalpies of Formation Revisited. *J. Phys. Chem. A* **2004**, *108*, 9979−9997.
(51) Changala, P. B.; Nguyen, T. L.; Baraban, J. H.; Ellison, G. B.; Stanton, J. F.; Bross, D. H.; Ruscic, B. Active Thermochemical Tables: The Adiabatic Ionization Energy of Hydrogen Peroxide. *J. Phys. Chem. A* **2017**, *121*, 8799−8806.
(52) https://atct.anl.gov/Thermochemical%20Data/version%201.122g/index.php (accessed January 18, 2021).
(53) Curtiss, L. A.; Raghavachari, K.; Redfern, P. C.; Pople, J. A. Assessment of Gaussian-2 and Density Functional Theories for the Computation of Enthalpies of Formation. *J. Chem. Phys.* **1997**, *106*, 1063−1079.
(54) Wagman, D. D.; Evans, W. H.; Parker, V. B.; Schumm, R. H.; Halow, I.; Bailey, S. M.; Churney, K. L.; Nuttall, R. L. The NBS Tables of Chemical Thermodynamic Properties. Selected Values for inorganic and C_1 and C_2 Organic Substances in SI units. *J. Phys. Chem. Ref. Data* **1982**, *11*, 2.
(55) Pyykkö, P. Additive Covalent Radii for Single-, Double-, and Triple-Bonded Molecules and Tetrahedrally Bonded Crystals: A Summary. *J. Phys. Chem. A.* **2015**, *119*, 2326−2337.

https://doi.org/10.1021/acs.jpca.2c06012
J. Phys. Chem. A 2022, 126, 7944−7953